

Quantum Phase Transitions in Anti-ferromagnetic Planar Cubic Lattices

Cameron Wallard¹ and Roman Oros²¹Centre for Quantum Computer Technology, School of Physics,
University of Melbourne, Victoria 3010, Australia.²Dept. d'Estructura i Constituents de la Materia, Univ. Barcelona, 08028, Barcelona, Spain.

(Dated: 9th February 2020)

Motivated by its relation to an NP-hard problem we analyze the ground state properties of anti-ferromagnetic Ising-spin networks in planar cubic lattices under the action of homogeneous transverse and longitudinal magnetic fields. We consider different instances of the cubic geometry and find a set of quantum phase transitions for each one of the systems, which we characterize by means of entanglement behavior and majorization theory. Entanglement scaling at the critical region is in agreement with results arising from conformal symmetry, therefore even the simplest planar systems can display very large amounts of quantum correlation. No conclusion can be made as to the scaling behavior of the minimum energy gap, with the data allowing equally good fits to exponential and power law decays. Analysis of entanglement and especially of majorization instead of the energy spectrum proves to be a good way of detecting quantum phase transitions in highly frustrated configurations.

PACS numbers: 03.67.-a, 03.65.Ud, 03.67.Lx, 03.67.Mn, 05.50.+q, 05.50.Fh

Quantum many bodied systems are of increasing interest in modern physics, particularly systems that exhibit a quantum phase transition (QPT). The nature of the quantum correlations between the components of these systems has been the subject of several recent studies [1, 2, 3, 4, 5, 6, 7, 8, 9, 10, 11, 12, 13, 14], with the suggestion that systems in the vicinity of the critical point are highly entangled. In this work we consider the phase structure of a spin model for which finding the ground state can, for certain parameters, be proven to belong to the complexity class NP-hard [15]. We detect the presence of a QPT between paramagnetic and anti-ferromagnetic phases and find that this transition is accompanied by a peak in the entanglement between different parts of the system with a scaling behavior that makes it hard to simulate classically [8, 14, 16, 17]. Additionally, for the simplest realization of the spin network, we have calculated the minimum energy gap for networks of up to $N = 24$ spins. The data accommmodates equally good fits to both exponential and power law decays, allowing no conclusion to be formulated as to the efficiency of adiabatic quantum algorithms in solving this classically NP-hard problem. Finally, we study the effects of frustration in these spin networks, which adds an extra element of complexity, altering the phase structure of the system.

The Hamiltonian under consideration is

$$H = \sum_{hi,ji} \frac{z}{i} \frac{z}{j} + B \sum_{i=1}^N \frac{z}{i} + \sum_{i=1}^N \frac{x}{i}; \quad (1)$$

where the sums over hi, ji and i run over the edges and vertices respectively of the particular lattice under study. The parameters B and x are respectively the longitudinal and transverse magnetic fields, and N is the number

of spins (qubits) each associated with an individual vertex of the lattice. Spin networks of various planar cubic geometries are considered, and a QPT between paramagnetic (large fields), and anti-ferromagnetic (low fields) phases is expected in each case, as shown in Fig.1

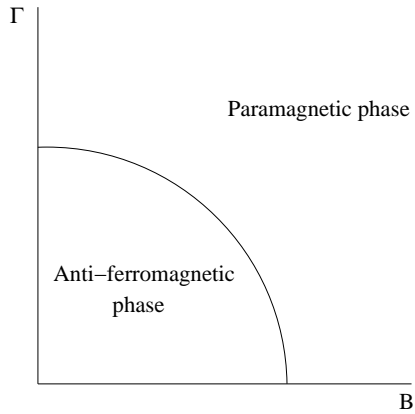


Figure 1: Expected phase diagram in the (B, Γ) plane for the system s under study.

For planar cubic lattices a ground state search of this system is NP-hard for the parameters $B = 1; \Gamma = 0$, however for extremely high fields, finding the ground state is clearly trivial, regardless of the size of the system. This gives rise to the possibility of performing the classically NP-hard ground state search using a quantum adiabatic algorithm. The procedure would be as follows: set the quantum register into the paramagnetic ground-state of the system, with a very large magnetic field, and adiabatically change this field to the values $B = 1; \Gamma = 0$. The system is guaranteed to evolve to the ground-state of this final Hamiltonian with a high probability. This involves crossing the phase boundary from the paramag-

netic phase to the anti-ferromagnetic stage, and the time required to perform the procedure is dependent on the energy spectrum at the transition point. Thus the structure of the QPT, and in particular the scaling behavior, can determine the computational cost of the adiabatic quantum algorithms of the type described above.

Initially we study the simplest planar cubic lattice, the "ladder on a circle" geometry from Fig 2, which consists of two coupled one-dimensional periodic spin chains. These lattices always contain an even number of nodes N , however they can be divided into two classes, those with an even number of nodes on each ring for which there is no frustration, and those which contain an odd number of nodes on each ring which do exhibit frustration.

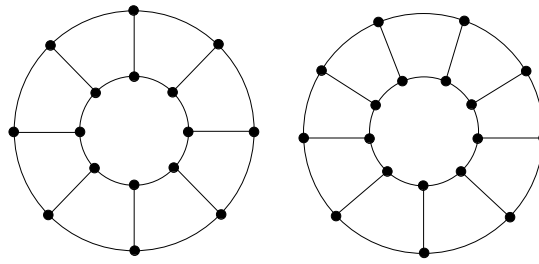


Figure 2: "Ladder on a circle" for $N = 16$ (left) and $N = 18$ (right). For $N = 16$ the system is not frustrated, while for $N = 18$ it exhibits frustration.

For the small lattice sizes we have considered ($N = 24$), the phase diagram of the system in the (β, γ) plane strongly depends on whether the system is frustrated or not. While for the non-frustrated instances a rich phase-structure was observed, with several clear indicators of a QPT, the transition for the frustrated system is more elusive. Clearly both systems must, in the thermodynamic (large N) limit, share the same phase diagram. Quantum phase transitions are marked by the vanishing of the first energy gap (ϵ_{12}), the difference between the ground-state and the first excited state energies. In the systems under study in this article this gap behaves as a possible order parameter, being finite in the paramagnetic phase while decreasing to zero for the antiferromagnetic phase in the thermodynamic limit.

Typically the existence of a quantum phase transition is also marked by a clear minimum in some other higher energy gap close to the critical point, which can be easily observed for finite systems. We detect this minimum in the second energy gap (ϵ_{13}) for the non-frustrated systems studied in this article, as is shown in Fig. 3 for the non-frustrated ladder with $N = 16$. In frustrated systems however, the multiple degeneracy of the ground-state in the antiferromagnetic phase implies that the minimum will only be manifest in some higher energy gap, making it far more difficult to observe.

The importance of the second energy gap ϵ_{13} lies also

in its role controlling possible adiabatic evolutions across the critical regions for non-frustrated ladders. In these systems, numerical analysis shows that there is no magnetic field term of the Hamiltonian between the ground and first excited states, therefore precluding a direct transition between these two states by adiabatically changing the magnetic fields. Consequently, it is not the first energy gap ϵ_{12} , but the second energy gap ϵ_{13} the one that determines the required evolution time of any adiabatic process across this set of quantum phase transitions.

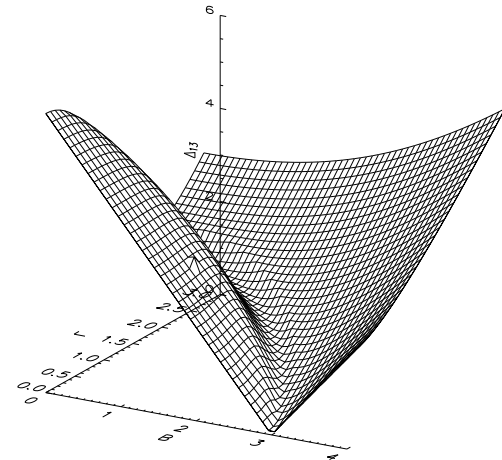


Figure 3: Phase diagram of the non-frustrated "ladder on a circle", for $N = 16$ spins. The energy gap between the ground and second excited state reveals the appearance of two well separated phases.

When moving between the two different phases, the ground state correlations of one particle with the rest of the system, as measured by the entanglement entropy $S(1)$, 1 being the reduced density matrix for a single spin, do not show any peak in the critical region. This single particle entanglement rises from zero in the paramagnetic region, to become maximal in the antiferromagnetic phase due the Z_2 symmetry of the system, which leads to degeneracy of the ground state in the $\beta = 0$ limit (e.g., the ground state for the "ladder geometry" is close to a GHZ state of N qubits in this limit). This fact leads to some numerical noise in the data. As any linear combination of degenerate eigenstates is also an eigenstate, some quantities, including entanglement measures, which are different for the different ground states, become ill-defined at this point, and depend on which state is chosen. Additionally, although actually non-degenerate for finite N , in larger systems the first energy gap may be too small for the diagonalization algorithm to resolve, leading similar problems for small values of N . This noise may be seen in some of the plots presented in this article, however wherever it is observed, the limiting behavior of the system is clear.

In contrast to the single particle entropy, the QPT is well-detected by the entropy of $N=2$ particles $S(N=2)$, $N=2$ being the reduced density matrix for $N=2$ spins, as seen in Fig.4. The entanglement between the exterior and the interior rings of the graph shows a peak at the critical points of the phase diagram. The QPT is therefore identified by a collective measure of entanglement, involving quantum correlations between large blocks of qubits.

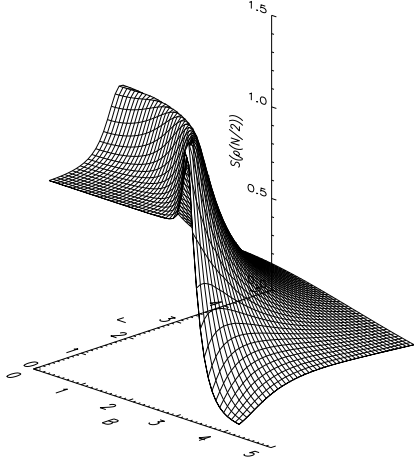


Figure 4: Entanglement entropy of the reduced density matrix for the particles on the inner (outer) ring, for $N = 16$. The peak indicates the crossing of the critical region in the $(B,)$ plane.

Scaling of this $N=2$ -particle entanglement at the critical region of the $(B,)$ plane with the size of the system seems to be in agreement with considerations from conformal symmetry, which predict a leading scaling behavior of $S(N=2) \propto N$ for our system, that is, entanglement entropy scales as the size of the boundary of the splitting, measured in terms of the number of qubits. Note that, despite the fact that our configuration is planar, the particular geometry we have chosen forces the scaling behavior of the entropy to be strongly linear, due to the linear number of short-range interactions we 'cut' with the bipartition between the inner and outer ring [4, 5, 8, 14, 18, 19, 20]. Simulations for non-frustrated lattices up to 24 qubits show that for the QPT across the $B = 1$ line, the entanglement entropy tends to obey $S(N=2) \approx 0.08N$ as the size of the system increases (see Fig.5). This behavior is similar to the linear law already found in [8] for the Exact Cover adiabatic quantum algorithm, and clearly differs from the logarithmic law found in [4, 5] for quantum spin chains. Entanglement scaling according to this particular bipartition of the system implies that even this simple planar model is able to produce an exponentially large amount of quantum correlations, as measured by the maximum rank of the reduced density matrices over all possible bipartitions, in such a way

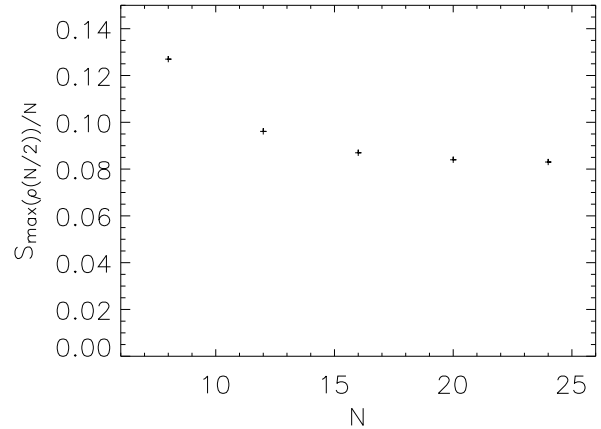


Figure 5: Maximum entanglement entropy per site between two rings of a non-frustrated ladder configuration as a function of the number of lattice sites, up to $N = 24$, along the line $B = 1$. For large N the quantity $\frac{S_{\max}(N=2)}{N}$ tends to a constant, which reveals an asymptotic linear scaling for the entropy peak.

that classical simulations of the transition and of possible adiabatic quantum algorithms would become efficient [8, 14, 16, 17].

Regarding the scaling behavior of the minimum value of the second energy gap, no definite conclusion can be extracted from our data for systems up to 24 qubits. As can be observed in Fig.6, where we plot the minimum energy gap along the $B = 1$ line as a function of the size of the system, we can not distinguish between exponential and power law decays for this quantity, as both of them are almost equally good. A definite determination of the scaling law in this case would involve the analysis of much bigger systems, which are clearly outside of our computational capabilities. As a consequence, no conclusion can be formulated as to the efficiency of possible adiabatic quantum algorithms in solving the NP-hard problem of determining the ground state of generic anti-ferromagnetic planar cubic systems with $B = 1$ and $= 0$ [15, 21].

Techniques from majorization theory [22, 23, 24, 25, 26] have proven to be fruitful in characterizing the structure of the ground state across a QPT. We have chosen to calculate the 2^N cumulants $c_1 = \sum_{i=1}^N p_i^{\#}$ arising from the sorted probabilities $p_i^{\#} = j_{ii} g_i j_i^2$ (where j_{ii} is a quantum state from the computational basis, j_{gi} is the ground state of the system, and $p_i^{\#}$ are the probabilities sorted into decreasing order) at each step when varying the Hamiltonian parameters. The majorization analysis of this set of probabilities has been useful in the study of efficiency in quantum algorithms [27, 28, 29]. Across the QPT on the line $B = 1$, we observe in Fig.7 that there

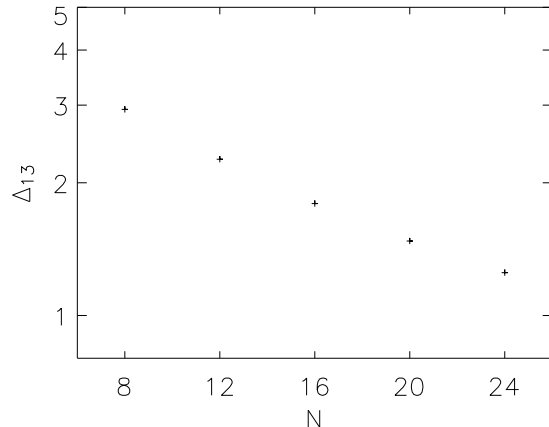


Figure 6: The top figure is a semi-log plot of the minimum value of the second energy gap along the $B = 1$ line as a function of the number of qubits, up to $N = 24$. Linearity of this plot would imply that gap decreases exponentially with the size of the system. The bottom figure is a log-log plot of the same data. Linearity of this plot would imply that the gap decreases as a power law with the size of the system. Both plots allow a linear fit with $R^2 > 0.99$ indicating that the scaling behavior of the energy gap requires the consideration of bigger systems to be determined consistently.

exist a majorization arrow in the direction of decreasing transverse magnetic field. The rapid growth of the cumulants starts precisely at the critical region, which indicates that this majorization analysis is sensitive to quantum phase transitions: such a sudden increase of the ground state cumulants in the same eigenbasis may be a signal of the presence of a critical point. Step-by-step majorization implies that the ground state is becoming increasingly ordered after each step in a very strong sense, at the precise level of each one of the probabilities, not just at the global level of expectation values, such as the mean magnetization. In frustrated ladders a second transition is observed, indicated clearly in the majoriza-

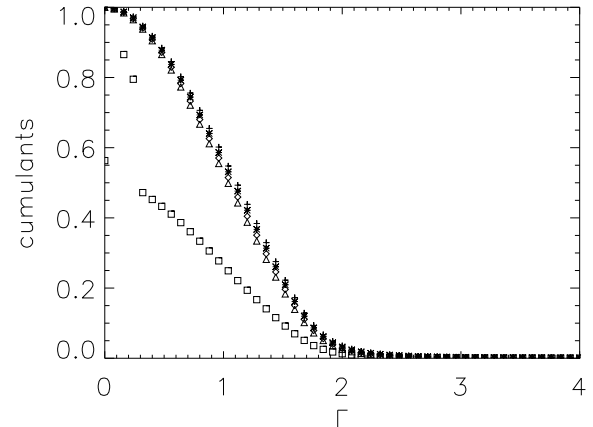


Figure 7: Majorization arrow for $B = 1$ when decreasing γ , for $N = 16$. There is a sudden change in the behavior of the cumulants at the critical point. For simplicity only the first five cumulants are plotted.

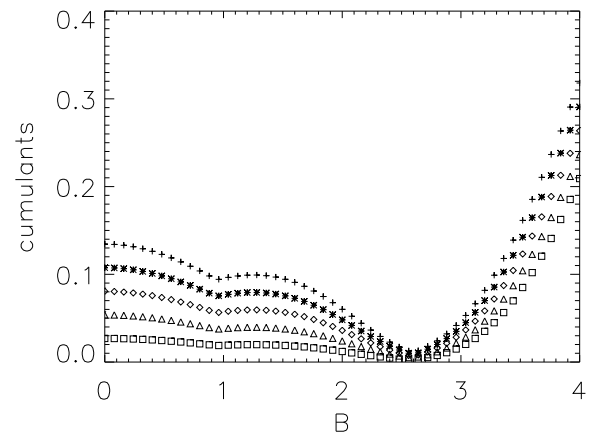


Figure 8: Majorization cumulants for the frustrated ladder lattice of $N = 14$ spins, for $\gamma = 1$ when decreasing B . Here a second transition is observed near $B = 1$, due to the frustration of the lattice. For simplicity only the first five cumulants are plotted.

tion curve from Fig.8, which is taken along the line $\gamma = 1$ again in the computational basis. This second transition is a result of the frustration in the system and, due to the high level of degeneracy of the ground-state in the region, is difficult to detect as a compression of energy levels, as shown in Fig.9, or as a peak in the entanglement entropy. Indeed even the onset of the transition at $B = 2.5$ is far more clear when looking at the majorization cumulants than the energy spectrum.

An alternative majorization analysis arises from the probability distribution obtained from the eigenvalues

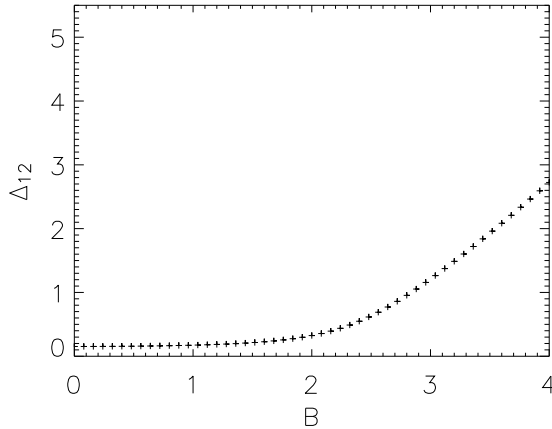


Figure 9: The first energy gap along the line $\Gamma = 1$ for a frustrated ladder of $N = 14$ spins fails to show the existence of a second phase transition near $B = 1$. Even the onset of the transition in the vicinity of $B = 2.5$ is not as clearly defined as in Fig.8.

of the reduced density matrix of $N=2$ particles. In the case of the "ladder" geometry this is obtained after tracing out one of the two rings. The behavior of the entanglement entropy implies that the disorder of this distribution is maximum at the critical point. An analysis in terms of the majorization cumulants reveals a change of behavior for most of the cumulants at the critical point, which reach their minimum values – corresponding to maximum disorder – and turn from step-by-step minorization to step-by-step majorization. This point seems to be a turning point for the lowest eigenvalue, where its second derivative is zero. This can be observed in Fig.10.

Other planar cubic lattices of different geometries show different behaviors of the phase diagram in the (B, Γ) plane. For example, we have analyzed the two geometries shown in Fig.11 (which we call "pentagonal" and "tetragonal" geometry) for $N = 20$ and $N = 16$ qubits respectively. These geometries are easily scalable, and for small instances, highly frustrated. The disappearance of the first energy gap at low values of the Hamiltonian parameters, as seen in Fig.12, indicates the presence of a QPT in the system. As opposed to the non-frustrated lattices no clear minimum can be observed in the second energy gap for this geometry. The transition can, however, also be detected in the study of the entanglement entropy for $N=2$ spins in the (B, Γ) plane, which reveals a sudden change in the structure of the ground state along a line separating low from high values of the magnetic fields, as shown in Fig.13 and Fig.14. This set of quantum phase transitions corresponds to a compression of the high energy levels of the system at the points at which correlations, as measured by the entanglement entropy,

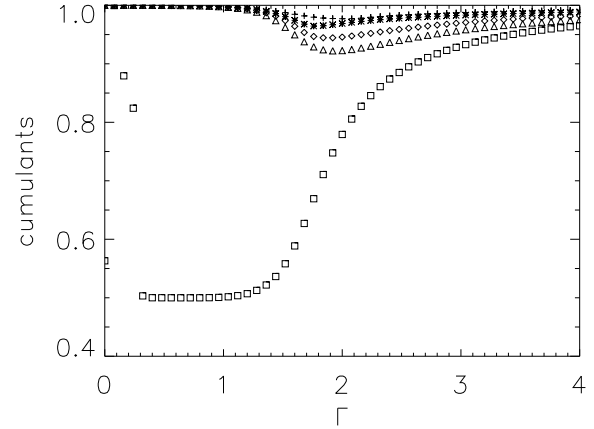


Figure 10: Majorization analysis of the eigenvalues of the density matrix $\rho_{N=2}$ when tracing out one of the rings, when decreasing Γ , for $N = 16$ and $B = 1$. There is a sudden change in the behavior of the cumulants at the critical point. For simplicity only the first five cumulants are plotted.

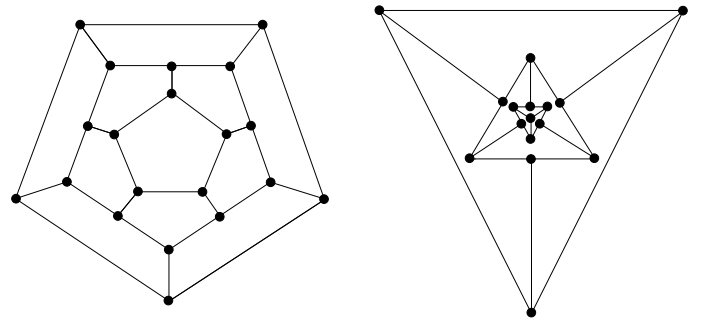


Figure 11: Pentagonal (left) and tetragonal (right) geometries for cubic planar lattices of $N = 20$ and $N = 16$ spins respectively.

are maximum [10].

The majorization analysis for these lattices reveals similar results to the ones presented for the "ladder" geometry: for $B = 1$ and when decreasing Γ the cumulants coming from the probabilities for the ground state of being in one of the computational states suddenly increase again at the critical point, as is observed in Fig.15 and Fig.16. Another signature of the QPT can be seen in the majorization behavior of the eigenvalues of the reduced density operator $\rho_{N=2}$ obtained when tracing out half of the system, which exhibit a minimum for some of the lowest cumulants at the critical point as is seen in Fig.17 and Fig.18.

To summarize, we have analyzed and characterized quantum phase transitions in anti-ferromagnetic planar cubic lattices under the action of homogeneous magnetic fields. We have shown that techniques from quantum in-

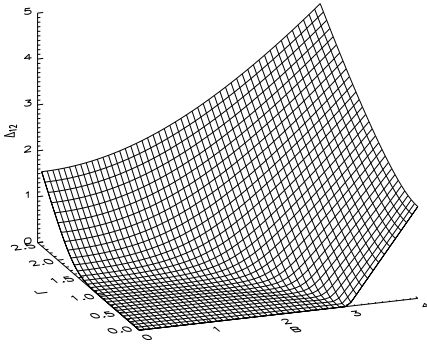


Figure 12: The 1st energy gap for the tetragonal geometry for $N = 16$. The disappearance of this energy gap is a clear indication of quantum phase transition.

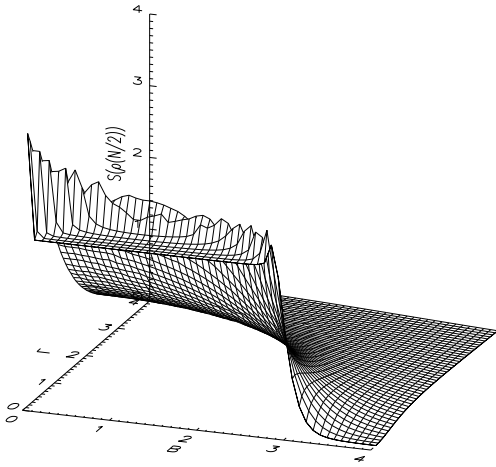


Figure 13: Entanglement entropy of $N = 2$ spins for the lattice of pentagonal geometry in the (B_1, B_2) plane, for $N = 20$. An abrupt change in the structure of the ground state is detected. Unavoidable numerical noise is present at low values of the magnetic fields.

formation science [30], such as the behavior of entanglement entropy or majorization theory, can be directly applied to the study of quantum many-body systems, leading to new points of view in the study of quantum critical phenomena. Lattices of different geometries present very rich phase diagrams with characteristic and differentiated anti-ferromagnetic and paramagnetic regions. Scaling laws for entanglement at the critical point seem to be in agreement with the laws predicted by conformal symmetry, in a way that even the simplest planar models are able to provide exponentially large quantum correlations, measured by the maximum rank of the reduced density matrices over all possible bipartitions. The understanding of the behavior of these systems is well characterized by the use of majorization theory and the analysis of entanglement entropy, both of which reveal details about

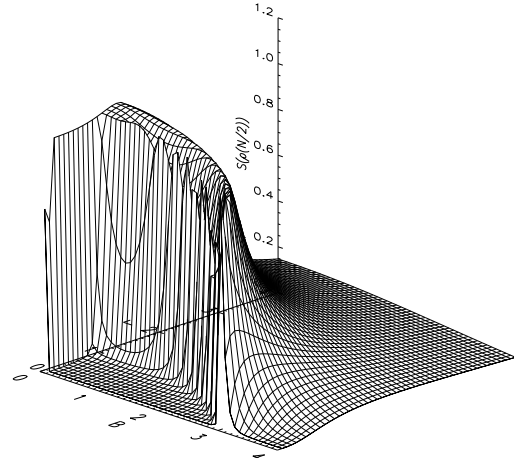


Figure 14: Entanglement entropy of $N = 2$ spins for the lattice of tetragonal geometry in the (B_1, B_2) plane, for $N = 16$. An abrupt change in the structure of the ground state is detected. Unavoidable numerical noise is present at low values of the magnetic fields.

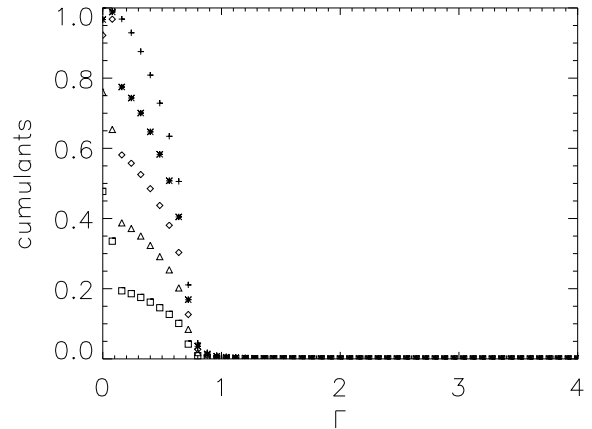


Figure 15: Majorization cumulants for the pentagonal lattice of $N = 20$ spins, for $B = 1$ when decreasing Γ . An abrupt change in their behavior is observed at the critical point. For simplicity only the first five cumulants are plotted.

the transitions present in the models which are sometimes hard to be obtained by the study of the energy spectrum.

Acknowledgments: R.O. acknowledges financial support from projects M C Y T F P A 2001-3598, G C 2001SGR-00065 and I S T -1999-11053. The authors are grateful to the Les Houches School of Theoretical Physics, where this work was initiated, and to discussions with L.C.L. Hollenberg, T.D. Kieu, N. Lambert, J. I. Latorre, A. Párs and E. Rico. Particular thanks to Wayne Hig (High Performance Computing System

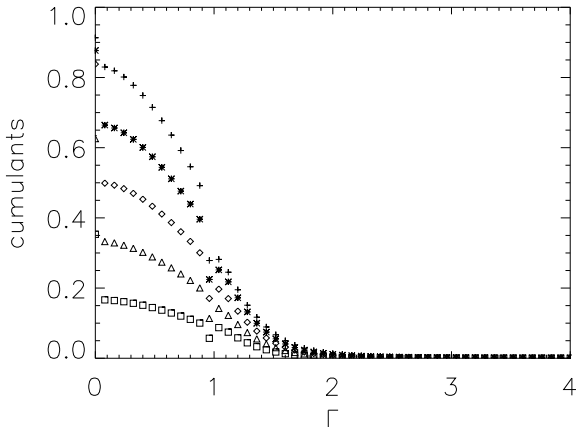


Figure 16: Majorization cumulants for the tetragonal lattice of $N = 16$ spins, for $B = 1$ when decreasing Γ . An abrupt change in their behavior is observed at the critical point. For simplicity only the first five cumulants are plotted.

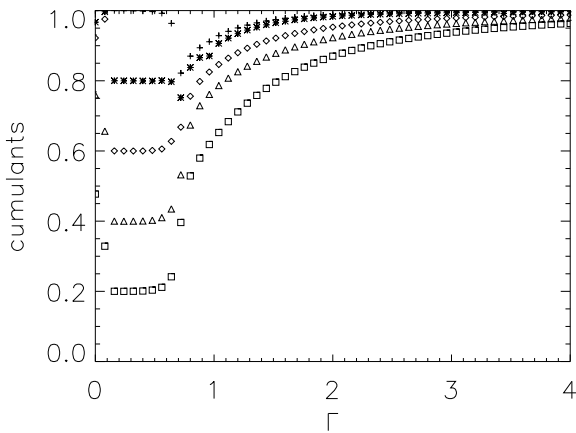


Figure 17: Majorization analysis of the eigenvalues of the density matrix $N=2$ when tracing out half of the system, when decreasing Γ , for $N = 20$ and $B = 1$ on the pentagonal lattice. There is again a sudden change in the behavior of the cumulants at the critical point. For simplicity only the first five cumulants are plotted.

Support Group, Department of Defence, Australia) for computational support.

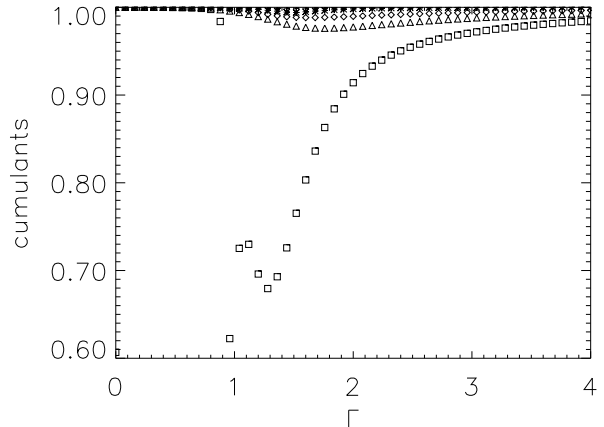


Figure 18: Majorization analysis of the eigenvalues of the density matrix $N=2$ when tracing out half of the system, when decreasing Γ , for $N = 16$ and $B = 1$ on the tetragonal lattice. There is a sudden change in the behavior of the cumulants at the critical point. For simplicity only the first five cumulants are plotted. Unavoidable numerical noise is present for the first cumulant close to $\Gamma = 1$.

Lett. 90, 227902 (2003), quant-ph/0211074.

- [5] J. I. Latorre, E. Rico, G. Vidal, quant-ph/0304098.
- [6] F. Verstraete, M. Popp, J. I. Cirac, quant-ph/0307009.
- [7] N. Lambert, C. Emery, T. Brandes, quant-ph/0309027.
- [8] J. I. Latorre, R. Orus, quant-ph/0308042.
- [9] V. Murg, J. I. Cirac, quant-ph/0309026.
- [10] H. L. Haselgrove, M. A. Nielsen, T. J. Osborne, quant-ph/0308083.
- [11] J. Vidal, R. Moessner, J. Dukelsky, cond-mat/0312130.
- [12] Olaf F. Syljuasen, quant-ph/0312101.
- [13] F. Verstraete, M. A. Martín-Delgado, J. I. Cirac, quant-ph/0311087 (accepted in Phys. Rev. Lett.).
- [14] R. Orus, J. I. Latorre, quant-ph/0311017.
- [15] F. Barahona, J. Phys. A: Math. Gen. 15, 3241-3253 (1982).
- [16] G. Vidal, Phys. Rev. Lett. 91, 147902 (2003), quant-ph/0301063.
- [17] G. Vidal, quant-ph/0310089.
- [18] C. G. Callan and F. Wilczek, Phys. Lett. B 333 (1994) 55, hep-th/9401072.
- [19] T. M. Fonda, J. Preskill, A. Strominger and S. P. Trivedi, Phys. Rev. D 50 (1994) 3987, hep-th/9403137; M. Srednicki, Phys. Rev. Lett. 71 (1993) 666-669, hep-ph/9303048.
- [20] D. K. Abbot and M. J. Strassler, Phys. Lett. B 329, 46 (1994), hep-th/9401125; D. K. Abbot, Nucl. Phys. B 453, 281 (1995), hep-th/9503016.
- [21] E. Farhi, J. Goldstone, S. Gutmann, M. Sipser, quant-ph/0001106.
- [22] R. F. Muirhead, Proc. Edinburgh Math. Soc. 21, 144, (1903).
- [23] G. H. Hardy, J. E. Littlewood, G. Polya, Inequalities, Cambridge University Press, 1978.
- [24] A. W. Marshall, I. Olkin, Inequalities: Theory of Majorization and its Applications. Academic Press Inc., 1979.
- [25] R. Bhatia, Matrix Analysis Graduate Texts in Mathematics, Springer-Verlag, Berlin, 1997.

matics vol. 169, Springer-Verlag, 1996.

[26] M .A .N ielsen, G .V idal, *Quantum Information and Computation*, 1, 76, (2001)

[27] J. I. Latorre, M .A .M art n-D elgado, *Phys. Rev. A* 66, 022305 (2002), quant-ph/0111146.

[28] R .O rus, J. I. Latorre, M .A .M art n-D elgado, *Quantum Information Processing*, 4, 283-302 (2003), quant-ph/0206134.

[29] R .O rus, J. I. Latorre, M .A .M art n-D elgado, quant-ph/0212094 (to appear in *The European Physical Journal D*).

[30] M .A .N ielsen, I. Chuang, *Quantum Computation and Quantum Information*, Cambridge University Press, 2000.